SYNTHESIS OF DRIVING SIGNALS FOR MEDICAL IMAGING ANNULAR ARRAYS FROM ULTRASONIC X-WAVE SOLUTIONS

L. Castellanos[1], A. Ramos and H. Calás
Dpto. Señales, Sistemas y Tecnologías Ultrasónicas, Instituto de Acústica - CSIC, Serrano 144, 28006 Madrid, Spain

Keywords: Beam Collimation, Driving signals, X wave, Pressure field, Velocity potential.

Abstract: An interesting approach for achieving high-resolution in ultrasonic imaging, is producing in real time limited diffraction waves with annular arrays; this potential option was presented by J.-Y. Lu in 1991 for collimating ultrasonic beams in medical imaging, approximating classical X waves with a finite aperture 10-annuli array, driven with 0-order X-wave excitation signal generated by solving the isotropic/homogeneous scalar wave equation. However, detailed solutions for a proper array electrical driving in order to form X-wave fields of both pressure and velocity potential have been not still reported. Paper objective is to show a tool to obtain approximated solutions for the inverse problems (aspect by-passed in classical approach) of synthesizing voltage excitations sets for producing both possible X wave field profiles, and comparatively investigate their distinct beam collimating capacities. All calculations, simulations and analyses were made for an ad-hoc developed 8-rings 2.5 MHz array transducer. Results show field distributions in ultrasonic pressure, created for two driving approaches derived by our inverse processing from calculated pressure and velocity potential fields. The good performances resulting in both cases for beam collimation, confirm the tool applicability. Results suggest the viability of our procedure as a promising alternative to classical X-wave driving calculations.

1 INTRODUCTION

To achieve with ultrasonic beams a high lateral resolution for medical imaging applications, requires conventional scanners with very complex electronic & processing technologies for performing a multiple focusing, of the classical phase-array type, or well to alternatively essay new ways for beam collimation, so searching a lower technological complexity. For this aim, some solutions based in non-diffracting set-ups have been proposed. One of the potentially best options seems to be the X waves, which are derived from theoretical limited-diffraction solutions for the scalar wave equation in isotropic/homogeneous media as is assumed in medical imaging. A classic practical approach for high-resolution was presented by J.-Y. Lu & J. F. Greenleaf in 1991 (Lu, 1991), which take the 0-order X waves as excitation signals for the multiple driving of an annular array. Other alternative kind of X waves were theoretically obtained by Shusilov *et. al.* (Shusilov, 2001), and Y. Crespo *et. al.* (Crespo, 2005), employing the method developed by Donelly *et. al.* (Donelly, 1992).

However, detailed solutions for a proper array electrical driving, by inverse processing, in order to form X-wave fields of both pressure and velocity potential, have been not still reported. The main paper objective is to overcome some aspects not addressed in classic X-wave approach: firstly to show in detail a reasonably approximated solution for the inverse problems of synthesizing voltage excitations sets, in order to produce X wave fields, and secondly to extent it for obtaining the 0-0rder X-wave in terms of pressure field pattern; in addition, the respective collimating properties of both field options are comparatively investigated.

2 THEORY

A. Potential Flow Theory

Potential flow theory describes the cinematic behaviour of the fluids. For this theory, it is assumed that the velocity field of flow is equal to the negative gradient of a potential function, this potential

Castellanos L., Ramos A. and Calás H. (2010).
SYNTHESIS OF DRIVING SIGNALS FOR MEDICAL IMAGING ANNULAR ARRAYS FROM ULTRASONIC X-WAVE SOLUTIONS.
In *Proceedings of the Third International Conference on Bio-inspired Systems and Signal Processing*, pages 290-295
DOI: 10.5220/0002746802900295

function cause the movement of the fluid, this is write like (Strutt, 1896):

$$\vec{u} = -\nabla\phi \quad (1)$$

Where: $\vec{u}$ is the velocity of vector for each medium particle, ϕ is the velocity potential field. In accordance with the potential flow theory, the pressure is describing like:

$$p = \rho_0 \frac{\partial\phi}{\partial t} \quad (2)$$

Where: p is the field of pressure, ρ_0 is the density of medium. Then the velocity potential is:

$$\phi = \frac{1}{\rho_0}\int p\,\partial t \quad (3)$$

B. Piezoelectric Transducer Model

A piezoelectric transducer is an especial kind of the electro-mechanic transducers. This transducer converting the electrical to mechanical energy and vice-versa, is employed like a sensor as an actuator.

The complexity of the electro-mechanic process is explicated with detail in some works (Masson, 1964), (Püttmer, 1997), (Arnau, 2004). The simplifications assumed for these analyses are based in the supposition of transducer working in only one vibration mode, and the planar dimensions of the piezoelectric material being larger than thickness. In this work, we employ an electric model of the Thickness Expander mode (*TE*) of the transducer. This model is based in SPICE piezoelectric model, developed by Püttmer *et. al.* (Püttmer, 1997).

C. Synthesizing approximated Voltage Excitations

To approach solutions to the inverse problems of synthesizing two voltage excitations sets, needs of describing the conversion of driving voltage V across input terminals to velocity u_L in the emitting face of transducer. For this, we take the following equation of transducer in broadband (Arnau, 2004):

$$V = \frac{h_{33}}{j\omega}u_L + \frac{h_{33}}{j\omega}u_B + \frac{1}{j\omega C_0^S}I \quad (4)$$

If we write the equation 4 in the time domain:

$$V = h_{33}\int u_L\,\partial t + h_{33}\int u_B\,\partial t + \frac{1}{C_0^S}\int I\ \partial t \quad (5)$$

Then, V could be approximated, in broadband operation, and under certain conditions in backing impedance u_B, as proportional to the integration of the velocity in the emitting face of transducer:

$$V \propto h_{33}\int u_L\,\partial t \quad (6)$$

D. Spatial Impulse Response Method

Spatial impulse response method (Stepanishen, 1971) has been largely applied to obtain the pressure field under a diffraction process. For array cases, the pressure response can be written as (Ullate, 1994):

$$p(x,t) = \rho\sum_{k=1}^{N}\frac{\partial(u_{Lk})}{\partial t} * h_k(x,t) \quad (7)$$

where p is the acoustic pressure, x is the vector of position, ρ is the density of medium, u_{Lk} is the velocity in the face of the annulus k, h_k is the spatial impulse response of the annulus k and * represent the time convolution operator.

E. Broadband 0-order X Wave Equation

Because the 0-order X wave allows a more punctual and effective collimation than other options among the X wave family, we use, as in (Lu, 1991), this sub-class. The expression for the 0-order X wave family produced by an infinite aperture and broadband conditions is (Lu, 1991):

$$\Psi_{X_0} = \frac{a_0}{\sqrt{(r\sin\zeta)^2 + [a_0 - i(z\cos\zeta - ct)]^2}} \quad (8)$$

where Ψ_{X_0} represents the theoretical 0-order X wave, $a_0 > 0$ is a constant, r is the radial coordinate, ζ ($0 < \zeta < \pi/2$) is the Axicon angle, z is the axial distance, c is the speed of sound in the medium, and t is the time. For our case, these parameter values were used: $a_0 = 0.05$ *mm*, $\zeta = 4°$ and c = 1.5 mm/μs.

2 DRIVING AND FIELD RESULTS

In this work, we consider two cases for the 0-order X waves: in pressure and in velocity potential.

The potential flow theory (Strutt, 1896) for field aspects, and expression (6) for inverse processing,

Table 1: Resume of field expressions from 0-order X-wave solution in terms of velocity potential.

	0-order X wave in velocity potential.
Theoretical pressure fields.	$-\frac{a_0 ic\rho_0\left[a_0 - i\left(z\cos\zeta - ct\right)\right]}{\left\{\left(r\sin\zeta\right)^2 + \left[a_0 - i\left(z\cos\zeta - ct\right)\right]^2\right\}^{3/2}}$
Theoretical potential velocity fields.	$\frac{a_0}{\sqrt{\left(r\sin\zeta\right)^2 + \left[a_0 - i\left(z\cos\zeta - ct\right)\right]^2}}$
Theoretical velocity fields.	$\frac{a_0 r\sin^2\zeta}{\left\{\left(r\sin\zeta\right)^2 + \left[a_0 - i\left(z\cos\zeta - ct\right)\right]^2\right\}^{3/2}}\vec{r} - \frac{a_0 i\cos\zeta\left[a_0 - i\left(z\cos\zeta - ct\right)\right]}{\left\{\left(r\sin\zeta\right)^2 + \left[a_0 - i\left(z\cos\zeta - ct\right)\right]^2\right\}^{3/2}}\vec{z}$
Signals $\propto$ to excitation voltages, derived by inverse processing .	$-\frac{h_{33}a_0\cos\zeta}{c\sqrt{\left(r\sin\zeta\right)^2 + \left[a_0 - i\left(z\cos\zeta - ct\right)\right]^2}} + K$

were employed to obtain the results shown in the table 1, which includes theoretical field expressions from X-wave solution in terms of velocity potential and an approximate driving voltage.

When a plane array transducer is modelled as vibrating in a thickness extensional (*TE)* mode, only is possible to calculate its perpendicular velocities field in the *z* direction. Thus, we only take into account velocities in *z* direction in order to obtain the proportional signals for the excitation voltages. As it is shown in table 1, our voltage excitations, to obtain 0-order X waves in velocity potential, are waveforms with morphology similar to excitation signals employed by J-Y Lu and J. F. Greenleaf in your X-wave experimental verification (Lu, 1991). To note that these approximated excitation signals are also very similar to the velocity potential.

Table 2: Geometrical characteristics of each transducer ring in the annular array transducer.

Number of element.	Intern Radio [mm].	Extern Radio [mm].	Evaluation value [mm].
1	0	2	0
2	2.2	4.59	3.395
3	4.79	7.2	5.995
4	7.4	9.81	8.605
5	10.01	12.4	11.205
6	12.6	15	13.8
7	15.2	17.6	16.4
8	17.8	20.3	19.05

In the figure 1, the normalized voltages with regard to the maximum are shown. These voltages are applied to each ring of the array transducer detailed in the table 2. Because these excitation voltages were obtained by means of the integration of the velocity fields taken toward propagation axis (*z*), we can displace these values of voltage on the horizontal axis with the addition of a constant *K*.

The voltages for the case of beam-forming with 0-order X-wave in pressure show that is necessary to generate a fast descending change with a rapid decay. While the lateral axis *x* (ring number) is increasing, figure 1.a shows that the value of decay is larger. It must be noted that only changes in the voltage signal excitations are relevant, because they provoke significant changes in the velocity of the particles on array transducers faces. The excitations voltages for the 0-order X wave in velocity potential show, in figure 1.b, two large changes as the more relevant for the generation of the velocities field.

Two sets of voltage driving were calculated (Figure 1), and applied to create the subsequent collimation patterns. The proposed method for this aim uses a broadband model (Püttmer, 1997), for the emission transfer functions in the annuli of the transducers array, combined with the potential flow theory. Acoustic field simulations use the general impulse response approach used for emitting arrays (Ullate, 1994). Differences between both synthesized ultrasonic beams are evaluated in the following for collimating purposes.

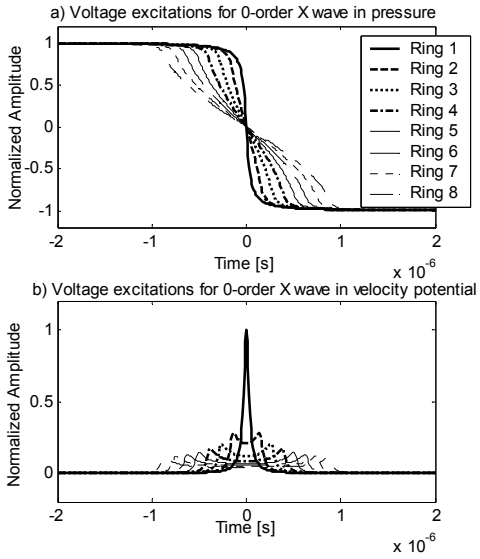

Figure 1: Voltage excitations to approximate beamforming of the 0-order X wave in: a) pressure, b) velocity potential.

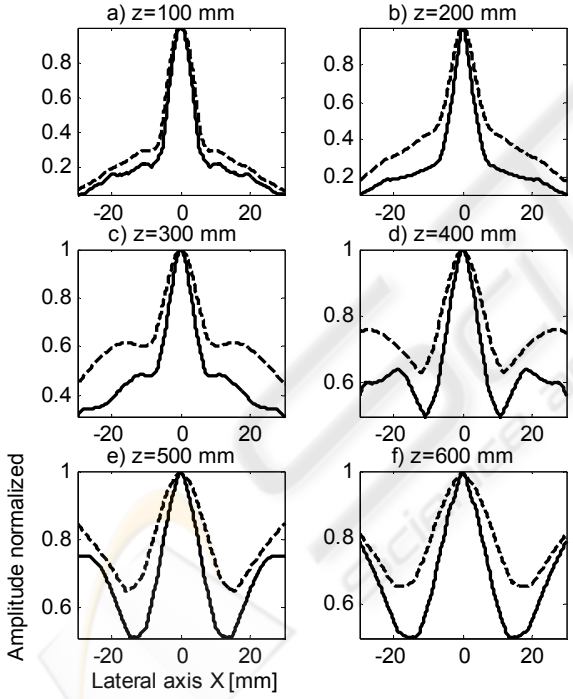

Figure 2: Normalized lateral axis 1-D profiles with regard to the maximum in each case, for two beam-forming approximations using the 0-order X wave expressions in pressure and velocity potential. The figure shows the beam profiles resulting in the pressure field, emitted by an ultrasonic annular array of 8-rings, for the case of using the X wave in pressure (dash line) and the X wave in velocity potential (continue line).

The figure 2 shows the lateral axis pressure profiles for the 0-order X waves expressed in pressure and velocity potential, in both cases in one dimension (1-D) and for distinct depths between 100 and 500 mm. In this figure, it is clearly show that for the case of using the expression of the velocity potential, the resulting sidelobes, from depths superior to 100mm, are quite smaller than in the case of using the pressure expression.

The figure 3 shows the axial pressure profiles normalized with regard to the maximum in both cases (driving derived from pressure and velocity potential expressions). In this figure, the case of using the X wave in pressure shows more uniform field amplitude, and in addition, the case of using the X wave in velocity potential originates a field decay with a certain ringing.

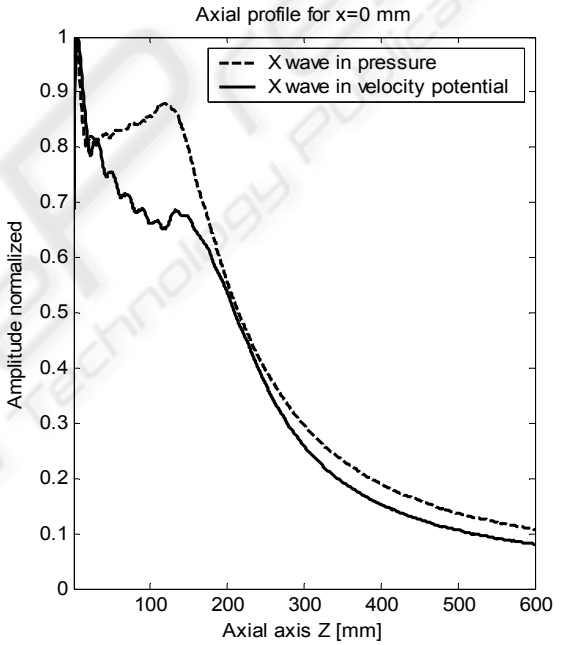

Figure 3: Morphology of axial pressure profiles normalized with regard to the maximum in each case, by approximating the beam-forming from the 0-order X waves in pressure (dash line), and velocity potential (continue line).

In relation to two-dimensional (2-D) field displays, figure 4 shows the spatial x-z distribution of the maxima amplitudes of the envelopes of the pressure field, normalized with regard to the display maximum in the two alternative cases (X wave expressions formulated in pressure and velocity potential terms). This figure shows that the pressure field when using for calculation the X wave in pressure is more stable than in the case of using the velocity potential. Furthermore, the case of using the

X wave in velocity potential produces a field with a narrower beamwidth and approximately with the same depth of field (measured at -6 dB) that when using pressure X wave, but showing some axial field ringing, with two discontinuous regions appearing in the -3 dB contour curve. This field ringing is due to the especial behaviour of the positive and negative regions in the pressure field signals (see figure 7).

And the figure 5 shows other type of 2-D display (space-temporal) of beamforming results by using the 0-order X waves in terms of pressure, and velocity potential, particularized for z = 100 mm, just a depth very usual in abdominal and cardiologic medical imaging. The resulting ultrasonic beam in this case, when the X wave expression in velocity potential is used, has two principal field maxima at the beginning of time axis, and some smaller secondary peaks afterwards, because of the strong diffraction effects in this zone. And, the case of using the X wave expression in pressure shows only one main maximum also with some secondary peaks, originated by the phenomenon of diffraction.

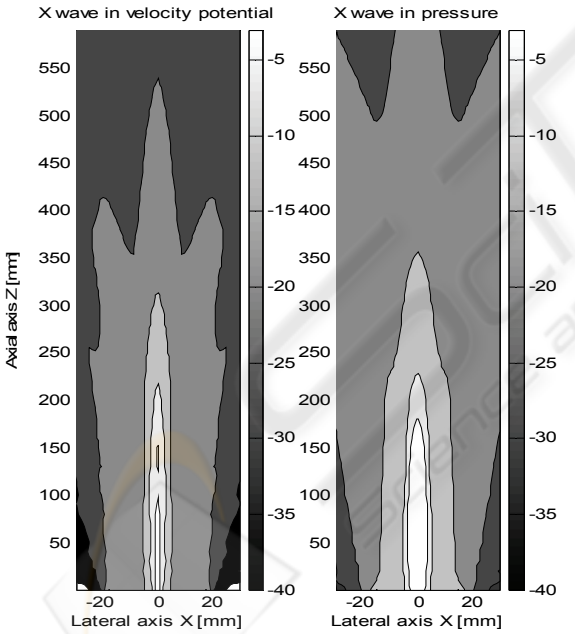

Figure 4: 2-D Display of the signal envelopes maxima in the pressure field, normalized with regard to the maximum in each case, for beam-forming approximation from the 0-order X waves in pressure and in velocity potential. The shown slices are in: -3 dB, -6 dB, -12 dB, -20 dB, -40 dB.

Figures 6-7 show waveforms in points of the x axis, obtained by a beamforming using 0-order X waves: in pressure and velocity potential.

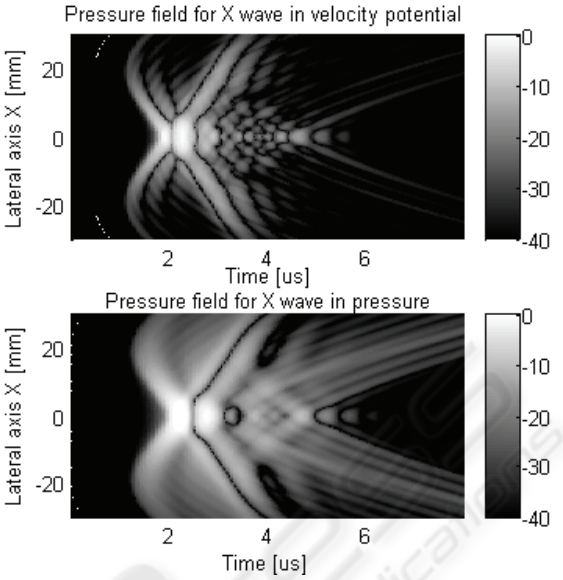

Figure 5: Pressure fields in spatial-temporal distribution, normalized with regard to the maximum in each 2-D display, by using 0-order X waves in pressure and velocity potential. The pressure field levels are shown in grey scale detailed in dB, for the axial distance z = 100 mm.

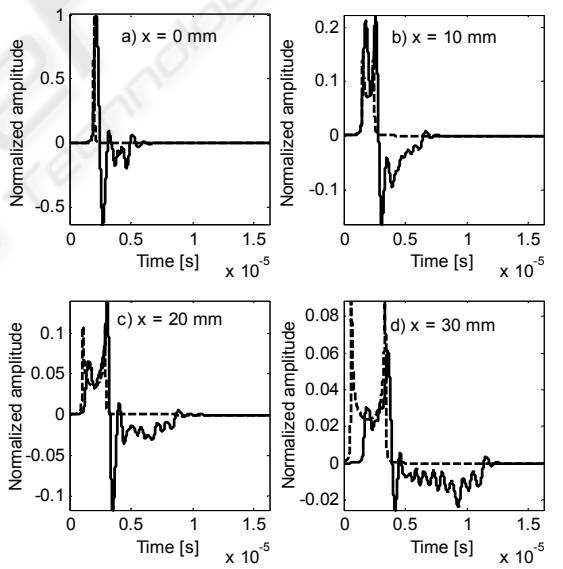

Figure 6: Pressure signal waveforms in x axis, at z = 100 mm, obtained with an annular array of 8-rings, normalized with regard to maximum, for beam-forming using the 0-order X wave in pressure (continue line) and the theoretical pressure field signals for X wave in pressure (dashes line).

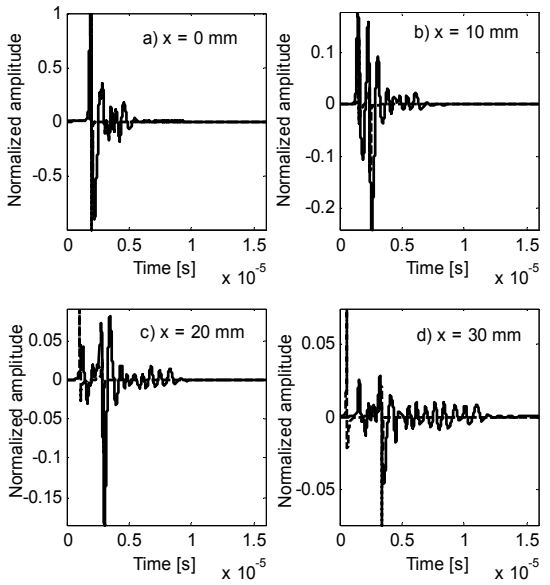

Figure 7: Pressure signal waveforms in x axis, at z = 100 mm, obtained with an annular array of 8-rings, normalized with regard to maximum, for beam-forming using the 0-order X wave in velocity potential (continue line), and theoretical pressure field signals for X wave in pressure (dashes line).

These figure show the time pressure signals for 4 points in the x axis, at a depth of z = 100 mm, obtained with an annular array of 8-rings, and the different signals are normalized with regard to the maxima signal amplitude. They show the similarity of signals morphology with the theoretical pattern for pressure field signals.

3 CONCLUSIONS

Results suggest that the procedure proposed in this paper by inverse processing from X-waves, as a tool for ultrasonic beam-forming analysis, creates new beam collimation options in high resolution medical imaging, constitutes a very useful and promising way to generate and evaluate beams alternatives to those derived from classical proposals to generate X-wave field distributions. And it could be also used for synthesizing special excitations of annular arrays to create other type of limited diffraction beams.

The good performance of the options evaluated here for beam focusing along certain field depths, potentiality confirms the suitability of the proposed tool. It seems also possible a successful application of it to synthesize the multiple driving needed for creating other types of high-resolution ultrasonic beams, also in terms of pressure, for future advanced bio-medical imaging equipment. As future work, it would be of quite interest, studying the effects of the ring widths, in the annular array, over the resulting beam properties, in order to optimize the morphology of the signals and of the field spatial distributions, and also to achieve a further reduction of the diffraction effects.

ACKNOWLEDGEMENTS

This work and the grant of Eng. L. Castellanos in CSIC (Videus lab) are being supported by the R&D National Plan of the Spanish Minister ‘‘Science & Innovation” (Projects: PN-DPI2005-00124 and PN-DPI2008-05213). The scientific stay of Dr. H. Calás in the Dpt. SSTU of the Acoustic Institute in Madrid is supported by Post-doctoral JAE Program (CSIC).

REFERENCES

Arnau, A., “Piezoelectric Transducer and Aplications”, Edit. Springer, ISBN 3-540-20998-0, 2004.

Crespo., Y., Calas H., Moreno E., Eiras J. A., Secada J. D., Leija L., “New X-wave solutions of isotropic/homogenous scalar wave equation”, ICEEE and CIE, IEEE Catalog Number: 05EX1097, ISBN: 0-7803-9230-2, p. 164-167, 2005.

Donnelly, R., Ziolkowski R., “A method for constructing solutions of homogeneous partial differential equations: localized waves”, Proc. R. Soc. Lond. A., No. 437, p. 673-692, 1992.

Lu, J. Y., Greenleaf, J. F., “Theory and Acoustic Experiments of Nondiffracting X Waves”, IEEE Ultrason. Symp. Proc., p. 1155, 1991.

Mason, W. P., “Physical Acoustics, Volume I-Part A”, Edit. Academic Press, 1964.

Püttmer, A., Hauptmannm P., Lucklum, R., Krause, O., Henning B., “SPICE model for lossy piezoceramic transducer”, IEEE Trans. Ultrason. Ferroelec. Freq. Contr., Vol. 44, No. 1, p. 60-66, 1997.

Stepanishen, P. R., “Transient radiation from pistons in an infinite planar baffle”, J. Acoust. Soc. Am., Vol. 49 (5B), p. 1629, 1971.

Strutt, J. W., “The Theory of Sound”, Vol. 2, Edit. MacMillian & Co., Second Edition, 1896.

Sushilov, Nikolai V., Tavakkoli, J., Cobbold R. S. C., “New X-wave solutions of free-space scalar wave equation and their finite size realization”, IEEE Transactions on Ultrasonics, Ferroelectrics, and Frequency Control, Vol. 48, No. 1, p. 274-284, 2001.

Ullate, L. G., Ramos, A., San Emeterio, J. L., “Analysis of the ultrasonic field radiated by time – delay cylindrically focused linear arrays”. IEEE Trans. Ultrason. Ferroelec. Freq. Control., Vol. 41, nº 5, p. 749-760, 1994.